Journal of Molecular Structure: THEOCHEM 960 (2010) 63–72

Contents lists available at ScienceDirect

Journal of Molecular Structure: THEOCHEM

journal homepage: www.elsevier.com/locate/theochem

Medium effect on the equilibrium geometries, vibrational frequencies and solvation energies of sulfanilamide

Mohammad A. Halim [a], Dawn M. Shaw [b], Raymond A. Poirier [a,*]

[a] Department of Chemistry, Memorial University, St. John's, NL, Canada A1B 3X7
[b] The Atlantic Computational Excellence Network, Memorial University, St. John's, NL, Canada A1B 3X5

ARTICLE INFO

Article history:
Received 6 July 2010
Received in revised form 18 August 2010
Accepted 23 August 2010
Available online 31 August 2010

Keywords:
Solvent effect
Sulfanilamide
Polarizable continuum model
Vibrational frequency
Solvation free energy

ABSTRACT

In this paper, the polarizable continuum model (PCM) is used to investigate the effect of solvent on the geometry, vibrational frequencies, IR intensities, Raman scattering activities, solvation free energies and the dipole moment of sulfanilamide. Hartee–Fock (HF), B3LYP and MP2 are employed for all models, both in gas phase and in solution, with basis sets up to 6-311+G(d,p) for HF and B3LYP and 6-31G(d) for MP2. A new SMD model is also used for solvation energy and dipole moment calculations. Some significant changes are observed in the dihedral angles but no noticeable changes appear in vibrational frequencies when sulfanilamide is solvated. Moreover, solvent effects on infrared intensities and Raman scattering activities are quite considerable and they increase as one goes from lower to higher dielectric constant. With PCM, both the solvation free energy and dipole moment of sulfanilamide increase when going from non-polar to polar solvents but no noticeable changes are observed among polar solvents. However, with SMD the solvation free energies are 15.5–33.0 kJ/mol and 9.6–19.7 kJ/mol higher than those of PCM for polar and non-polar solvent, respectively.

1. Introduction

Theoretical investigations of vibrational spectra are generally conducted with an isolated molecule in the gas phase, however, the experimental studies most often involve molecules in solution, so there is a need to account for solvent effects in theoretical approaches. For many years, IR and Raman spectroscopies were widely used as standard tools for structural characterization of molecular systems by quantum-chemical calculations [1]. The effect of solvent on the molecular vibrational (IR and Raman) spectra can be successfully explained by the environmental factors that affect the vibrational frequency, the intensity and the band shape [2]. Furthermore, solvent effects are a pivotal tool for drug design in the pharmaceutical industry because they affect the release, transport and degree of absorption of the drug in the organism, which is important for future development and formulation efforts of the drug.

It is a long-term challenge in computational chemistry to deal with solvation effects accurately and efficiently [3]. Although there are many solvation models to describe the condensed-phase system, they can broadly be divided into two main groups. The first group includes simulation methods which are based on the parameterization of the force field and explicit treatment of solvent molecules [4,5]. The second group includes implicit solvation models (also called continuum solvation models), where the discrete structure of the solvent is neglected [6,7]. Continuum solvation models are becoming more and more popular [8,9] as effective tools to extend the quantum-chemical description of molecular energies, structures, and properties of systems in solution [10]. The polarizable continuum model [11] has many advantages and among them two are quite significant: reduction of the number of degrees of freedom for molecular systems and accurate treatment of the strong, long-range electrostatic forces [5].

Sulfa drugs, which are derivatives of sulfanilamide, have been an integral part of our medical history. They were the first effective chemotherapeutic agents to be widely used for the treatment of bacterial infection in humans and animals [12]. In 1932, a German biochemist, Gerhard Johannes Paul Domagk (1895–1964) first tested the sulfa drug, Prontosil, on his daughter who was near death from a streptococcal infection in her arm and had failed to respond to other treatments. Her arm was subsequently restored to full health after the treatment [13]. Sulfanilamide, first used in 1936, was the grandparent of the sulfonamide family of drugs that are still in use today. Moreover, the discovery of sulfanilamide greatly reduced the mortality rate during World War II. After the first uses of sulfanilamide, nearly 30 years later an experimental vibrational frequency study was performed by Mueller [14]. Recently, the first [15] computational IR study on sulfanilamide was

* Corresponding author. Tel.: +1 709 864 8609; fax: +1 709 864 3702.
E-mail addresses: mahalim@mun.ca (M.A. Halim), michelles@mun.ca (D.M. Shaw), rpoirier@mun.ca (R.A. Poirier).

0166-1280/$ - see front matter Crown Copyright © 2010 Published by Elsevier B.V. All rights reserved.
doi:10.1016/j.theochem.2010.08.027

performed using HF/3-21G and later IR and Raman studies [16] were extended using HF/6-21G(d). In 2007, a combined experimental and computational study using B3LYP and the 6-31++G(d,p) basis set for the infrared spectra of sulfanilamide and its azanions was conducted [17]. However, no detailed study employing solvent has been performed on the structure, spectra and solvation free energies of sulfanilamide. In this study, the effect of solvent medium has been investigated in detail with three levels of theories and six different basis sets.

2. Computational methods

All calculations were carried out with the Gaussian09 software package [18]. The geometries were fully optimized and the frequencies (all values are in harmonic approximation) were calculated in the gas phase and with different solvents (water, dimethyl sulfoxide, and chloroform) at the HF and B3LYP levels of theory using 6-31G(d), 6-31G(d,p), 6-31+G(d), 6-31+G(d,p), 6-311G(d) and 6-311+G(d,p) basis sets and at MP2/6-31G(d). For geometries, vibrational frequencies, solvation free energies and dipole moment calculations the polarizable continuum model, which is the default in Gaussian09, was used. For solvation free energy (ΔG_{sol}) and dipole moment, we also applied a new continuum solvation model based on the charge density of the solute molecule interacting with a continuum solvent called SMD (solvation model on density) developed by the Truhlar group in 2009 [19]. In addition, seven solvents were included for solvation free energies and dipole moment calculations. Frequencies were scaled using the scale factors summarized in Table 1 for all level of theories and basis sets employed [20]. The absence of imaginary frequencies confirmed that the stationary points correspond to minima on the Potential Energy Surface. In total there are 51 vibrations and the assignments of the calculated wave numbers were aided by the animation option of the program GaussView [21].

3. Results and discussion

3.1. Equilibrium geometries

To study the vibrational frequencies, it is essential to examine the geometry of any compound as small changes in geometry can potentially cause substantial changes in frequencies. Although the solute–solvent interactions are less crucial than the intramolecular forces, the geometry of the solute does undergo important changes in going from the gas phase to solution [22]. In this study, though we performed all geometry optimizations in gas and condensed media with all the basis sets mentioned in the methods section, only 6-31G(d), 6-31+G(d,p) and 6-311+G(d,p) basis sets are presented here with HF and B3LYP, and 6-31G(d) with MP2. The structure of sulfanilamide is shown in Fig. 1. The structure of the sulfanilamide has also been studied using HF/3-21G, HF/6-21G(d), MM and B3LYP/6-31++G(d,p) [15–17].

The theoretical and experimental [17,23] (X-ray diffraction) bond lengths (Å) are compared in Table 2. Overall, the HF/6-311+G(d,p) bond lengths are in good agreement with both experimental results A and B. Generally, it is expected that the bond distances calculated by electron correlated methods are longer than the experimental distances, however, in this study only the MP2/6-31G(d) C–H and N–H bond distances are longer than the experimental values. All non-hydrogen bond distances (C–S, S–O, S–N and C–C), except for C–N with B3LYP, are longer than the experimental results. The mean absolute deviation (MAD) of bond lengths from experiment (A) [23] for HF/6-31G(d), HF/6-31+G(d,p) and HF/6-311+G(d,p) are 0.083, 0.082, and 0.082 Å, respectively whereas with B3LYP and the same basis sets they are 0.098, 0.098, and 0.090 Å, respectively. The MAD value for MP2/6-31G(d) is 0.097 Å. Interestingly, all calculated bond lengths are significantly longer than the experimental bond distances where hydrogen is present. For example, C(3)–H(14), C(4)–H(13), C(6)–H(9), and C(7)–H(8) bond distances are 0.143–0.156, 0.166–0.178, 0.156–0.168, and 0.234–0.247 Å longer respectively than the experimental values. The nitrogen–hydrogen bond distances in the amino and amido groups of sulfanilamide vary notably compared to experiment (A). For instance, compared to the experimental values the calculated amino N(10)–H(11) and N(10)–H(12) bond distances are longer by 0.244–0.264 and 0.114–0.134 Å respectively whereas, the amido N(15)–H(16) and N(15)–H(17) bond distances are 0.239–0.260 and 0.169–0.190 Å, respectively. The considerable differences in N–H bond distances are not due to the theoretical shortcomings since experimental results are also subject to variations due to insufficient data to calculate the equilibrium structure and which are sometimes averaged over zero-point vibrational motion [24]. In an X-ray structure the error in the position of the hydrogen atoms is such that their bonding parameters greatly vary compared to the non-hydrogen atoms. In addition, the error associated with the hydrogen is not unusual in X-ray structures [23], especially for compounds containing 'heavy' atoms like the sulfur contained in sulfanilamide. Intermolecular hydrogen bonding is also an important factor in the crystalline state of sulfanilamide which usually leads to shortening of the N–H bond.

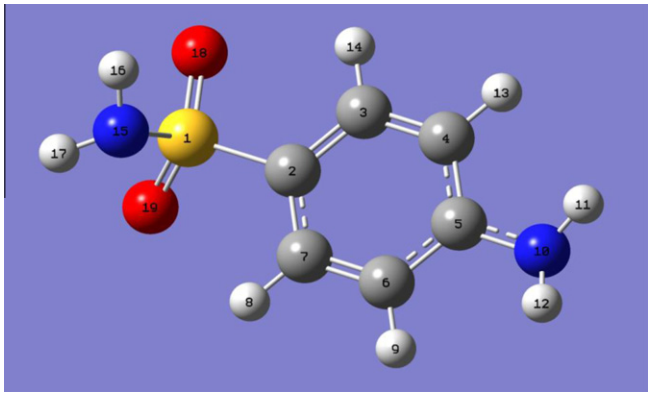

Fig. 1. Structure of sulfanilamide.

Table 1
Scaling factor suitable for vibrational frequencies.[a]

Basis sets	HF	B3LYP
6-31G(d)	0.8953	0.9613
6-31G(d,p)	0.8992	0.9627
6-31+G(d)	0.8970	0.9636
6-31+G(d,p)	0.9007	0.9648
6-311G(d)	0.9013	0.9672
6-311+G(d,p)	0.9059	0.9688

[a] Ref. [19], 0.9441 for MP2/6-31G(d).

The calculated and experimental bond angles are presented in Table 3. Significant differences are observed in the calculated C2–S1–N15, C5–N10–H12, S1–N15–H16, and S1–N15–H17 bond angles compared to other experimental values. The calculated C2–S1–N15 and S1–N15–H17 bond angles are 4.5–7.3° and 5.0–7.5° smaller, respectively than the experimental results whereas the calculated C5–N10–H12 and S1–N15–H16 bond angles are 2.4–5.6° and 5.5–8.0° larger than the experimental results, respectively. All the other bond angles are reasonably close to the experimental results. The MAD values of calculated bond angles from experiment (A) in HF/6-31G(d), HF/6-31+G(d,p), and HF/6-311+G(d,p) are 1.9, 1.4, and 1.5 and B3LYP using 6-31G(d),

Table 2
Theoretical (gas phase) and experimental (X-ray diffraction) bond distances (Å) of sulfanilamide.

Bond distances	6-31G(d)			6-31+G(d,p)		6-311+G(d,p)		Expt (A)[a]	Expt (B)[b]
	HF	B3LYP	MP2	HF	B3LYP	HF	B3LYP		
S(1)–C(2)	1.755	1.779	1.765	1.758	1.782	1.756	1.783	1.751	1.743
S(1)–N(15)	1.655	1.706	1.688	1.650	1.703	1.650	1.701	1.608	1.635
S(1)–O(18)	1.433	1.469	1.467	1.433	1.470	1.426	1.463	1.443	1.454
S(1)–O(19)	1.432	1.467	1.465	1.433	1.470	1.426	1.463	1.425	1.430
C(2)–C(3)	1.386	1.397	1.395	1.388	1.398	1.385	1.394	1.391	1.395
C(2)–C(7)	1.391	1.399	1.397	1.388	1.398	1.388	1.395	1.379	1.402
C(3)–C(4)	1.381	1.389	1.392	1.380	1.390	1.379	1.387	1.377	1.382
C(3)–H(14)	1.073	1.085	1.086	1.074	1.085	1.074	1.083	0.930	–
C(4)–C(5)	1.394	1.408	1.403	1.398	1.410	1.395	1.406	1.396	1.409
C(4)–H(13)	1.076	1.087	1.088	1.076	1.087	1.076	1.085	0.910	–
C(5)–C(6)	1.400	1.410	1.406	1.398	1.410	1.398	1.407	1.384	1.393
C(5)–N(10)	1.381	1.386	1.396	1.380	1.386	1.381	1.384	1.381	1.388
C(6)–C(7)	1.375	1.387	1.389	1.380	1.390	1.376	1.386	1.381	1.377
C(6)–H(9)	1.076	1.087	1.088	1.076	1.087	1.076	1.085	0.920	–
C(7)–H(8)	1.074	1.085	1.087	1.074	1.085	1.074	1.083	0.840	–
N(10)–H(11)	0.996	1.011	1.014	0.995	1.009	0.994	1.008	0.750	–
N(10)–H(12)	0.996	1.011	1.014	0.995	1.009	0.994	1.008	0.880	–
N(15)–H(16)	1.001	1.019	1.020	1.000	1.017	0.999	1.015	0.760	–
N(15)–H(17)	1.002	1.019	1.020	1.000	1.017	0.999	1.015	0.830	–
MAD[c]	0.083	0.098	0.097	0.082	0.098	0.082	0.095		

[a] Ref. [23].
[b] Ref. [17].
[c] MAD value using Expt(A).

Table 3
Theoretical (gas phase) and experimental (X-ray diffraction) bond angles of sulfanilamide.

Bond angles	6-31G(d)			6-31+G(d,p)		6-311+G(d,p)		Expt[a]
	HF	B3LYP	MP2	HF	B3LYP	HF	B3LYP	
C2–S1–N15	104.3	103.5	102.8	105.6	104.5	104.5	104.2	110.1
C2–S1–O18	107.6	107.6	107.5	107.9	107.9	107.9	107.7	106.7
C2–S1–O19	109.4	108.9	108.7	107.9	107.9	107.9	108.1	108.5
N15–S1–O18	109.0	108.9	109.2	106.4	106.4	106.4	107.3	106.3
N15–S1–O19	104.7	104.7	105.0	106.4	106.4	106.4	105.9	106.5
S1–C2–C3	120.2	119.9	119.7	120.0	119.8	119.8	119.8	119.7
S1–C2–C7	119.8	119.7	119.4	120.0	119.8	119.8	119.7	120.6
C3–C2–C7	120.0	120.4	120.8	120.0	120.4	120.4	120.5	119.7
C2–C3–C4	120.1	119.8	119.4	120.1	119.8	119.8	119.7	119.8
C3–C4–C5	120.4	120.6	120.7	120.4	120.6	120.6	120.7	121.0
C4–C5–C6	119.0	118.8	118.9	119.0	118.8	118.8	118.7	118.5
C4–C5–N10	120.6	120.7	120.5	120.5	120.6	120.6	120.6	120.1
C6–C5–N10	120.3	120.5	120.3	120.5	120.6	120.6	120.6	121.5
C5–C6–C7	120.4	120.6	120.7	120.4	120.6	120.6	120.7	120.8
C2–C7–C6	120.1	119.8	119.4	120.1	119.8	119.8	119.7	120.2
C5–N10–H11	116.2	116.5	114.4	116.8	117.6	117.6	117.4	117.0
C5–N10–H12	116.2	116.5	114.4	116.8	117.6	117.6	117.4	112.0
S1–N15–H16	112.0	109.6	110.2	111.7	109.5	109.5	110.1	104.0
S1–N15–H17	110.0	107.5	108.1	111.7	109.5	109.5	109.3	115.0
MAD	1.9	1.8	1.9	1.4	1.5	1.5	1.6	

[a] Ref. [23].

6-31+G(d,p) and 6-311+G(d,p) basis sets are 1.8, 1.5, and 1.6°, respectively, and 1.9° for MP2/6-31G(d). Graphical comparisons (Fig. 2) of calculated and experimental bond lengths and bond angles indicate that MP2/6-31G(d) show significant variation with experiment.

The effect of medium on the molecular geometry of the sulfanilamide was investigated with PCM. Changes in geometrical parameters are significant when going from the gas phase to solution. The average change, $\overline{\Delta g}$, of the bond distances, bond angles, and dihedral angles is summarized in Table 4. It can be seen from Table 4 that a higher average change ($\overline{\Delta g}$) is observed in dihedral angles as compared to bond distances and angles. Significant changes, as seen in Table 5, are observed in the dihedral angles of D1–D12 where they range from 3.1° to 45.9°. Among all dihedral angles, the largest deviations are observed for O18–S1–N15–H16 and O18–S1–N15–H17. For example, the smallest variation in O18–S1–N15–H16 (15.5°) occurs in a non-polar solvent at HF/6-31G(d) whereas the largest variation (45.0°)occurs in water at B3LYP/6-31+G(d,p). For O18–S1–N15–H17, these same variations are 16.2° for chloroform at HF/6-31G(d) and 45.9° for water at B3LYP/6-31+G(d,p), respectively. Overall, the average change of geometrical parameters gradually increases from chloroform to DMSO but there is no consistent trend from DMSO to water. Therefore, comparing the different sets of geometrical parameters, it can be concluded that dihedral angles are more affected by solvent effect than bond distances and angles.

3.2. Vibrational frequencies in gas phase

All calculated frequency values presented in this paper are obtained within the harmonic approximation which allows us to describe vibrational motion in terms of independent vibrational

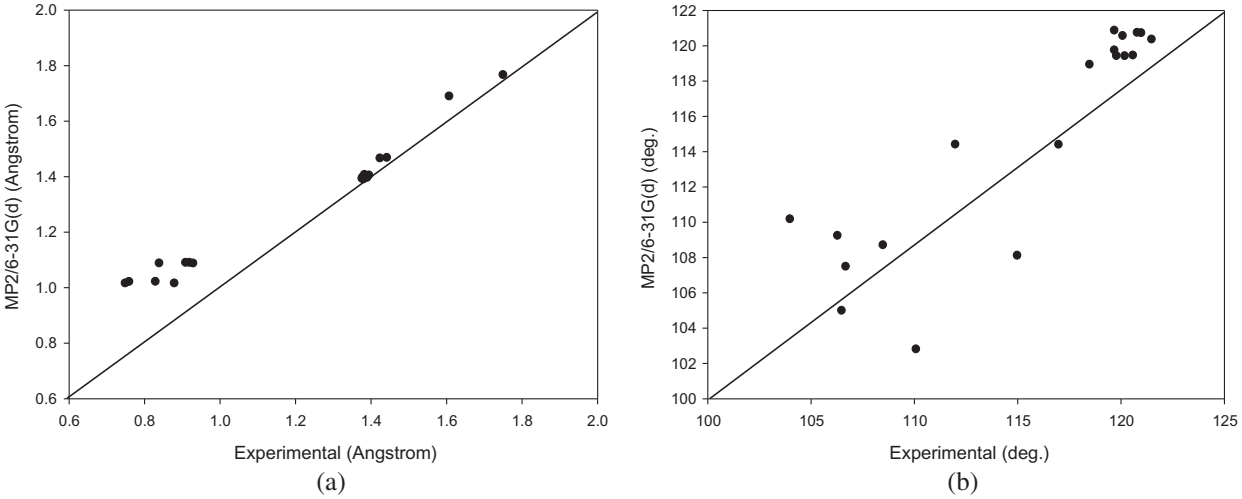

Fig. 2. Comparison of theoretical (gas phase) and experimental (X-ray) (a) bond distances (Å) and (b) angles (°) of sulfanilamide.

Table 4
Average change ($\overline{\Delta g}$) for geometrical parameters of sulfanilamide when going from the gas phase to solution.

	Bond distance (Å)			Bong angle (°)			Dihedral angle (°)		
	ϵ = 4.7	ϵ = 46.8	ϵ = 78.3	ϵ = 4.7	ϵ = 46.8	ϵ = 78.3	ϵ = 4.7	ϵ = 46.8	ϵ = 78.3
HF/6-31G(d)	0.002	0.003	0.003	0.3	0.4	0.4	3.3	4.0	4.0
B3LYP/6-31G(d)	0.003	0.004	0.004	0.5	0.6	0.6	14.2	41.7	41.7
MP2/6-31G(d)	0.002	0.003	0.003	0.4	0.5	0.5	67.8	60.0	60.0
HF/6-31+G(d,p)	0.003	0.004	0.004	0.7	0.7	0.7	26.7	27.3	18.3
B3LYP/6-31+G(d,p)	0.003	0.004	0.004	0.6	0.8	0.8	27.1	45.9	63.8
HF/6-311+G(d,p)	0.003	0.004	0.004	0.5	0.6	0.6	24.2	24.8	33.7
B3LYP/6-311+G(d,p)	0.003	0.004	0.004	0.6	0.7	0.7	25.8	62.4	62.4

modes each of which is governed by a simple one-dimensional harmonic potential. A comparison of calculated and experimental vibrational frequencies for sulfanilamide is presented in Table 6 which shows that even after scaling, large frequency shifts (above 50 cm^{-1}) are observed for ν_{18}, ν_{31}, ν_{34}, ν_{48}, ν_{49}, ν_{50}, and ν_{51}. The largest frequency shift, 161 cm^{-1}, corresponds to the amido NH_2 asymmetrical stretch. The calculated vibrational frequencies for asymmetrical stretching modes of amino and amido NH_2 are observed in the region 3481–3578 and 3432–3504 cm^{-1} and the symmetrical stretching modes appear in the region 3376–3475 and 3318–3398 cm^{-1}, respectively. These values are somewhat higher than the expected values of 3250–3480 cm^{-1} for amino and 3230–3390 cm^{-1} for the same stretching modes in the amido NH_2 group [25]. An experimental study by Topacli [12] reported that the bands at 3474 and 3372 $cm^{-1}$are assigned to the asymmetric and symmetric stretching of amino NH_2 and relatively lower at 3350 and 3261 cm^{-1} for the asymmetric and symmetric stretching of amido NH_2, respectively. In our study, the asymmetric and symmetric stretching modes of amino NH_2 agree reasonably well with the experimental results.

However, the calculated asymmetric and symmetric stretching modes of amido NH_2 are higher than the experimental [17] result (71–151 cm^{-1} in symmetrical and 89–161 cm^{-1} in asymmetrical) which is inconsistent with the difference found for the calculated N–H bond distances. This provides further evidence that errors in the experimental N–H distance are longer than for other bond distances. Overall, the vibrational frequencies of NH_2 calculated with the correlated MP2 method using 6-31G(d) basis sets are closer to both experimental (A and B) frequencies than those at HF and B3LYP with 6-31G(d), 6-31G(d,p), 6-31+G(d,p) and 6-311+G(d,p). The stretching modes for CH are usually expected [25] in the region 3005–3115 cm^{-1} in very close agreement with this study (3013–3107 cm^{-1}). As this paper's focus is on the effect of solvent on vibrational modes, a detailed mode by mode comparison will not be included.

The Mean Absolute Percentage Deviation (MAPD) of calculated unscaled and scaled frequencies from experiment [17] is presented in Table 7. For scaled frequencies, HF/6-311G(d) provides a better account of low-frequencies (<1000 cm^{-1}) than either B3LYP or MP2. The MAPD value for low-frequencies is 3.0% at HF/6-311G(d) and 8.2% at B3LYP/6-31+G(d,p). For the high-frequencies (>1000 cm^{-1}), all calculated MAPD results are in the range of 1.6–2.6%. For unscaled low and high-frequencies, the MAPDs are nearly the same for B3LYP using different basis sets and fell in the range 3.4–5.8%. For HF, this range is 8.0–11.5%. For unscaled vibrations, both HF and B3LYP theories using 6-31+G(d) basis sets provide relatively higher MAPD values than the other basis sets used in this study. Overall, the errors for the unscaled vibrational frequencies calculated using HF are large compared to the frequencies calculated using B3LYP. One reason is that HF overemphasizes the bonding and it makes the force constant large and subsequently the frequencies are overestimated. However, in this study the scaling factor dramatically improves the performance of HF frequencies analogous to what was found in a similar study [26].

3.3. Solvent effect on frequencies, IR intensities, and Raman activities

Average changes in unscaled vibrational frequencies are presented in Table 8 and IR intensities and Raman activities in Table 9 for sulfanilamide in going from the gas phase to different dielectric media. Comparison of vibrational frequencies, IR intensities and Raman activities (obtained at zero-frequency limit) for gas phase and solution (in water) are shown in Fig. 3. For IR intensities, scaling factor 0.63 is applied in gas phase at HF with all basis sets, however,

Table 5
Selected dihedral angles (°) that changed significantly in going from gas phase to continuum.

		6-31G(d)			6-31+G(d,p)		6-311+G(d,p)	
		HF	B3LYP	MP2	HF	B3LYP	HF	B3LYP
ϵ = 78.3								
N15–S1–C2–C3	D1	5.7	13.7	13.7	18.6	23.0	13.6	20.0
N15–S1–C2–C7	D2	5.8	12.8	12.8	18.5	22.3	13.7	19.8
O18–S1–C2–C3	D3	3.1	10.6	10.6	13.8	17.5	9.9	15.3
O18–S1–C2–C7	D4	3.1	9.7	9.7	13.6	16.8	10.0	15.1
O19–S1–C2–C3	D5	6.0	13.5	13.5	17.1	20.9	13.2	18.8
O19–C1–C2–C7	D6	6.1	12.6	12.6	17.0	20.3	13.3	18.6
C2–S1–N15–H16	D7	18.8	23.5	23.5	41.9	43.2	29.9	36.0
C2–S1–N15–H17	D8	19.2	23.1	23.1	43.9	44.1	31.3	36.9
O18–S1–N15–H16	D9	20.2	24.7	24.7	43.5	45.0	31.5	37.8
O18–S1–N15–H17	D10	20.6	24.3	24.3	45.4	45.9	32.9	38.6
O19–S1–N15–H16	D11	17.9	22.2	22.2	40.5	41.7	28.5	34.4
O19–S1–N15–H17	D12	18.3	21.7	21.7	42.5	42.5	30.0	35.2
ϵ = 46.8								
N15–S1–C2–C3	D1	5.8	13.7	17.8	19.0	23.0	13.8	20.0
N15–S1–C2–C7	D2	5.8	12.8	15.3	18.8	22.3	13.9	19.8
O18–S1–C2–C3	D3	3.1	10.6	14.8	14.2	17.5	10.2	15.3
O18–S1–C2–C7	D4	3.2	9.7	12.3	14.0	16.8	10.2	15.1
O19–S1–C2–C3	D5	6.0	13.5	17.6	17.5	21.0	13.4	18.8
O19–C1–C2–C7	D6	6.1	12.6	15.1	17.3	20.3	13.5	18.6
C2–S1–N15–H16	D7	18.6	23.3	22.5	41.7	43.0	29.7	35.9
C2–S1–N15–H17	D8	19.0	22.9	22.4	43.7	43.9	31.1	36.7
O18–S1–N15–H16	D9	20.0	24.5	23.6	43.2	44.8	31.2	37.5
O18–S1–N15–H17	D10	20.4	24.1	23.4	45.2	45.7	32.6	38.4
O19–S1–N15–H16	D11	17.7	22.0	21.3	40.3	41.5	28.3	34.2
O19–S1–N15–H17	D12	18.1	21.6	21.1	42.3	42.4	29.7	35.1
ϵ = 4.7								
N15–S1–C2–C3	D1	5.6	14.0	18.1	20.5	22.0	14.4	19.1
N15–S1–C2–C7	D2	5.5	12.9	15.5	19.8	21.2	14.1	18.7
O18–S1–C2–C3	D3	3.7	11.6	15.8	16.5	17.4	11.5	15.2
O18–S1–C2–C7	D4	3.6	10.6	13.1	15.7	16.6	11.1	14.9
O19–S1–C2–C3	D5	5.7	13.6	17.7	18.9	19.9	13.8	17.7
O19–C1–C2–C7	D6	5.6	12.6	15.1	18.2	19.0	13.5	17.3
C2–S1–N15–H16	D7	14.6	19.4	18.8	36.8	38.1	25.2	31.3
C2–S1–N15–H17	D8	15.3	19.2	18.7	38.7	39.2	26.7	32.3
O18–S1–N15–H16	D9	15.5	20.2	19.4	37.9	39.3	26.2	32.4
O18–S1–N15–H17	D10	16.2	19.9	19.4	39.8	40.4	27.7	33.5
O19–S1–N15–H16	D11	13.8	18.3	17.6	35.6	36.8	24.0	29.9
O19–S1–N15–H17	D12	14.5	18.0	17.6	37.5	37.9	25.4	30.9

Table 6
Selected vibrational frequency shifts (cm^{-1}) from experimental (KBr) to calculated (gas phase).

Mode	6-31G(d)			6-31G(d,p)		6-31+G(d)		6-31+G(d,p)		6-311G(d)		6-311+G(d,p)		Expt.[a] (ν)
	HF	B3LYP	MP2	HF	B3LYP	HF	B3LYP	HF	B3LYP	HF	B3LYP	HF	B3LYP	
ν_{18}	−54	−69	−81	−59	−68	−59	−72	−76	−76	−53	−67	−65	−75	703
ν_{23}	9	−16	−24	10	−17	12	−18	12	12	9	−15	12	−18	826
ν_{24}	−26	−44	−71	−28	−55	−29	−61	−34	−34	−21	−52	−33	−72	899
ν_{27}	−12	−17	−22	−8	−18	−6	−19	−4	−4	−13	−13	−5	−13	1003
ν_{30}	−3	−29	−23	−11	−40	−4	−34	−14	−14	−6	−17	−7	−40	1097
ν_{31}	−50	−45	−29	−51	−46	−47	−57	−53	−53	−34	−46	−54	−58	1146
ν_{33}	−13	−18	−20	−14	−22	−14	−17	−15	−15	−12	−15	−14	−20	1188
ν_{34}	−106	−29	−43	−104	−28	−107	−47	−106	−106	−105	−34	−109	−46	1312
ν_{37}	−19	−7	51	−15	−9	−20	−9	−21	−21	−16	−13	−18	−18	1336
ν_{38}	−9	−15	−18	−7	−17	−12	−18	−11	−11	−7	−13	−11	−21	1438
ν_{39}	0	−14	−25	2	−17	−2	−17	−1	−1	1	−15	0	−22	1505
ν_{40}	36	9	4	15	−18	36	12	15	15	39	16	23	−12	1549
ν_{41}	15	−5	−5	18	−7	14	−7	15	15	37	19	18	−9	1573
ν_{42}	9	−4	−7	12	−8	5	−8	8	8	18	−4	9	−13	1600
ν_{43}	11	−8	−16	−2	−24	15	−6	−2	−2	36	12	2	−25	1638
ν_{48}	110	100	71	136	122	124	121	148	148	152	148	151	150	3247
ν_{49}	37	58	2	66	83	36	67	68	68	74	94	73	101	3374
ν_{50}	114	110	89	149	137	127	131	161	161	150	154	152	157	3343
ν_{51}	43	68	19	82	103	39	76	83	83	76	104	80	114	3462

[a] Ref. [17].

the use of a scaling factor is less applicable for DFT intensities [27]. In order to make better comparison with gas phase, the infrared intensities in solution are divided by refractive index of the respective solvents [28]. For chloroform, the highest average change of the overall frequencies is observed at B3LYP/6-311+G(d,p) and the lowest at B3LYP/6-31G(d). In DMSO, HF/6-31+G(d,p) provides the larg-

Table 7
MAPD values of vibrational frequencies (gas phase) of sulfanilamide calculated from experiment[a].

	6-31G(d)			6-31G(d,p)		6-31+G(d)		6-31+G(d,p)		6-311G(d)		6-311+G(d,p)	
	HF	B3LYP	MP2	HF	B3LYP	HF	B3LYP	HF	B3LYP	HF	B3LYP	HF	B3LYP
Scaled (overall[b])	2.6	3.6	4.4	2.7	4.1	3.2	4.8	3.5	5.4	2.7	3.9	3.4	5.2
Unscaled (overall)	10.7	3.6	4.5	9.9	3.7	10.2	9.6	9.6	4.4	10.6	3.8	9.4	4.4
Scaled (low[c])	3.2	5.5	7.2	3.3	6.1	4.4	7.6	4.8	8.2	3.0	5.7	4.5	8.0
Unscaled (low)	9.7	3.4	3.5	8.6	4.1	9.0	8.0	8.0	5.7	9.7	3.8	8.3	5.8
Scaled (high[d])	2.0	1.6	1.6	2.2	2.1	2.0	2.0	2.3	2.6	2.4	2.0	2.3	2.5
Unscaled (high)	11.5	3.7	5.5	11.1	3.5	11.3	10.9	10.9	3.4	11.4	3.7	10.4	3.1

[a] Ref. [17].
[b] Overall, all frequencies.
[c] Low, frequencies <1000 cm^{-1}.
[d] High, frequencies >1000 cm^{-1}.

est change whereas HF/6-31G(d) and B3LYP/6-31G(d) contribute the smallest change. There is no large change observed in vibrational frequencies for DMSO or water except for HF/6-31+G(d,p). Although one would expect that the presence of dielectric medium has a strong influence on the theoretical frequencies, our results revealed that the dielectric medium has no significant effect on vibrational frequencies as we can see from Fig. 3a for water. The effects of *p*-polarization functions on hydrogen and diffuse functions on heavy atoms (6-31G(d) → 6-31+G(d,p)) and increasing the basis set from double-ζ valence to triple-ζ valence (6-31+G(d,p) → 6-311+G(d,p)) are not noticeable for a non-polar solvent. In dimethyl sulfoxide ($\epsilon = 46.8$), addition of polarization functions on hydrogen and diffuse functions on heavy atoms slightly increases the frequencies at HF and B3LYP. Moreover, triple-ζ valence has no significant impact on the average frequency changes for all solvents employed. Average changes for vibrational frequencies increase slightly in going from non-polar to polar solvent, however, there is no noticeable change for DMSO or water.

Detailed comparisons between the theoretical and experimental study for the IR and Raman spectra of sulfanilamide with water and DMSO could not be made because of the lack of experimental data. A comparison of experimental high-frequencies of sulfanilamide in $CDCl_3$ [17] with calculated high-frequencies in $CHCl_3$, however, revealed that relatively large deviations are observed in unscaled frequencies for HF and small changes for B3LYP and MP2 regardless of the basis sets. In addition, scaled frequencies show better performance regardless of the level of theory and basis sets and only the comparison with HF/6-31G(d) is presented in Fig. 4.

IR intensities are expected to dramatically change when the solute is solvated and this is indeed the case in our present study. A graphical presentation of IR intensities between gas phase and polar (water) condensed media is shown in Fig. 5. In chloroform, noticeable changes are observed in ν_{13}, ν_{14} intensities at HF and B3LYP with 6-31G(d), and also at HF/6-311+G(d,p). In addition, significant IR intensity changes are observed for the ν_{32}, ν_{35}, ν_{36}, ν_{42}, ν_{43} vibrational frequencies, though it is not consistent with all theories and basis sets. In the non-polar solvent, the smallest change is observed at MP2/6-31G(d) (18.21 km/mol) and the largest change appears at HF/6-31G(d) (37.00 km/mol). It seems that in the non-polar solvent ($\epsilon = 4.7$), the basis set has a strong influence on the average change in IR intensities as reported by density functional theory and it increases as one goes from smaller to larger basis set. On the other hand, using HF theory, it significantly decreases from 6-31G(d) to 6-31+G(d,p) and slightly increases from 6-31+G(d,p) to 6-311+G(d,p). In both polar solvents, the largest IR intensity change is observed at B3LYP/6-311+G(d,p) which is shown in Fig. 3b for water. Addition of diffuse and polarization functions in the basis set increased the IR intensities by about 3.06 km/mol whereas addition of triple-ζ valence for HF slightly decreased the same intensities. However, in the case of results reported from DFT, addition of more functions to the basis set gradually increased the IR intensities.

Like IR intensities, significant changes in Raman activities (obtained at the zero-frequency limit) are observed when sulfanilamide is solvated (Fig. 6). Average changes in Raman scattering activities in non-polar and polar solvent are not consistent with the increase of basis set size for the HF result but it gradually increases for B3LYP. For the non-polar and polar solvents, the smallest change is observed for HF/6-31G(d) and the largest change appears for B3LYP/6-311+G(d,p). A comparison of Raman scattering activities between gas phase and water is shown in Fig. 3c. Most important scattering activities are observed at the ν_{42}–ν_{51} vibrational modes which revealed that Raman peaks are strong for asymmetric and symmetric stretching modes of amido and amino NH_2 as well as stretching modes of CH regardless of the theories and basis sets used. Some Raman activities are notably inconsistent. For example, in chloroform the ν_{36} Raman peak is strong for HF with all basis sets but relatively weak for B3LYP and MP2, while ν_{32} is strong for HF and MP2 but very weak for B3LYP. On

Table 8
Average change for unscaled vibrational frequencies (cm^{-1}) of sulfanilamide in going from gas phase to solution.

	Overall[a]	$\epsilon = 4.7$			$\epsilon = 46.8$			$\epsilon = 78.3$	
		Low[b]	High[c]	Overall	Low	High	Overall	Low	High
HF/6-31G(d)	10.0	8.2	11.8	8.2	6.2	10.0	8.2	6.2	10.2
B3LYP/6-31G(d)	6.3	6.6	6.6	8.2	8.9	7.6	8.3	8.9	7.7
MP2/6-31G(d)	7.5	9.2	5.9	9.1	10.2	7.9	9.1	10.3	8.1
HF/6-31+G(d,p)	10.0	10.1	9.8	15.5	10.9	20.0	11.6	9.7	13.4
B3LYP/6-31+G(d,p)	9.8	11.2	8.4	11.6	12.2	11.1	11.7	12.2	11.3
HF/6-311+G(d,p)	9.1	9.2	9.0	10.9	9.4	12.4	10.0	9.3	12.5
B3LYP/6-311+G(d,p)	10.1	12.1	8.1	11.9	13.4	10.5	12.0	13.4	10.7

[a] overall, all frequencies.
[b] Low, frequencies <1000 cm^{-1}.
[c] High, frequencies >1000 cm^{-1}.

Table 9
Average change in IR intensities[a] (km/mol), and Raman activities (A^{-4}/amu) of sulfanilamide from gas phase to solution[b].

	ϵ = 4.7		ϵ = 46.8		ϵ = 78.3	
	IR Int.	Ram. Act.	IR Int.	Ram. Act.	IR Int.	Ram. Act.
HF/6-31G(d)	37.00	17.86	32.14	27.24	39.38	27.81
B3LYP/6-31G(d)	24.41	22.57	30.20	35.67	37.02	36.43
MP2/6-31G(d)	18.21	22.28	22.05	35.11	25.36	35.86
HF/6-31+G(d,p)	30.50	19.43	35.73	30.61	43.44	31.76
B3LYP/6-31+G(d,p)	36.67	27.46	43.70	43.77	35.97	44.76
HF/6-311+G(d,p)	31.88	19.17	35.66	30.68	42.87	31.38
B3LYP/6-311+G(d,p)	36.67	30.01	44.41	44.09	50.10	44.97

[a] All HF IR intensities in gas scaled by 0.63.
[b] IR intensities in solution divided by respective refractive index of solvent (H_2O = 1.3330, DMSO = 1.4793, $CHCl_3$ = 1.4458).

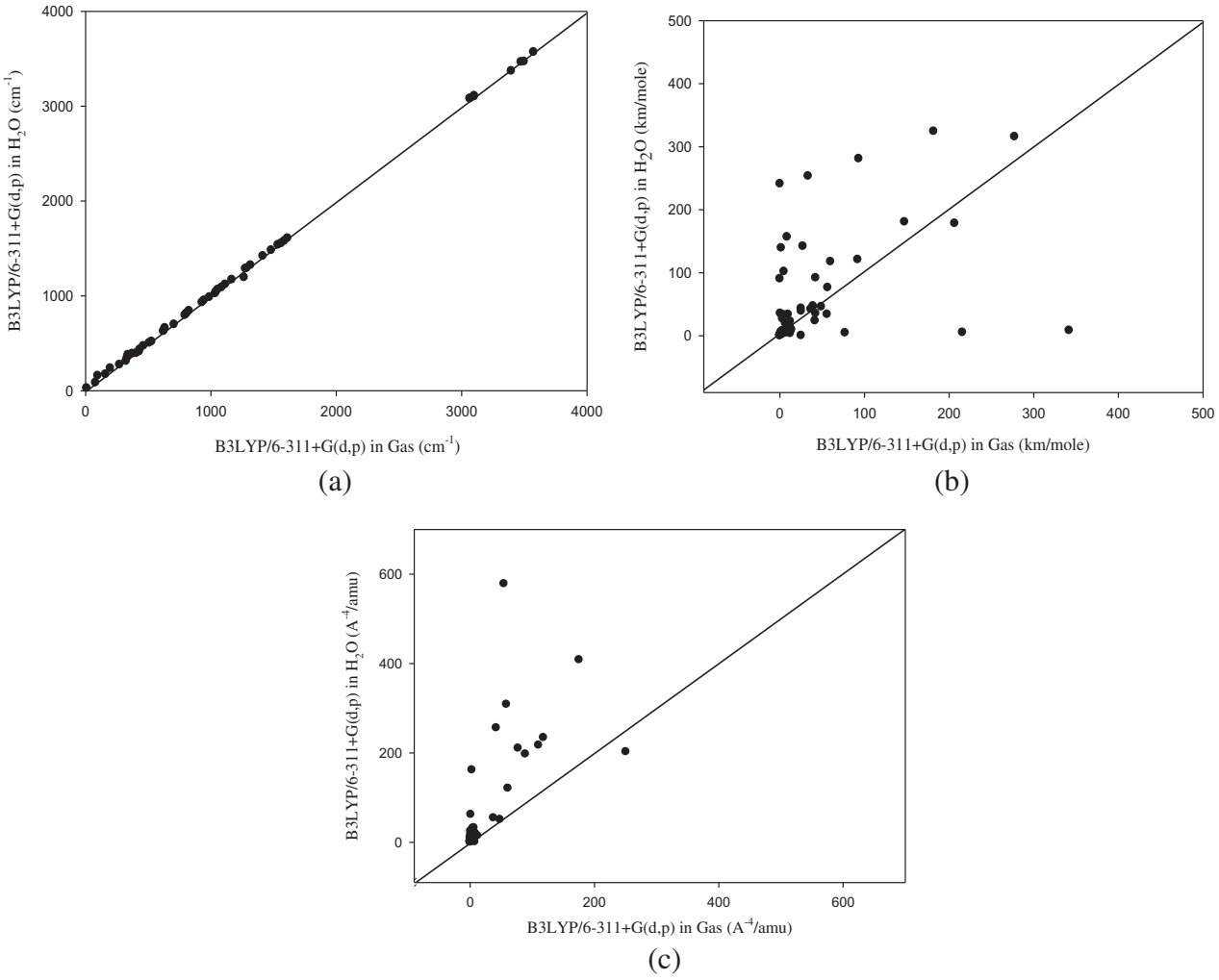

Fig. 3. Comparison of gas phase and water (a) frequency (cm^{-1}), (b) IR intensities (km/mole), and (c) Raman activities (A^{-4}/amu) of sulfanilamide.

the other hand, the Raman activity of ν_{23} is strong at B3LYP and MP2 but very weak at HF.

3.4. Solvation free energy and dipole moment

The most important properties of any chemical system (solute) with the surrounding solvent can best be described by means of free energy variation [29]. In PCM, [2] the solute–solvent interaction energies are described by four terms; electrostatic, dispersions, repulsions, and cavitations supplemented by a fifth term called thermal motion (tm). However, in SMD [19], the standard-state solvation free energy contribution is quite different, including electronic, nuclear and polarization components (ENP); cavitations, dispersions, and solvent structure change (CDS); and concentration change between the standard state of gas phase and condensed-phase in the energy term. In this study, we compare the PCM and SMD models, with the latter one being a recommended model for solvation free energy calculation in Gaussian09. Only the calculated solvation free energies (ΔG_{sol}) are summarized in Table 10 as no experimental data was found for sulfanilamide. For all levels of theory, the solvation energies steadily increased in going from lower to higher dielectric constant for PCM but no

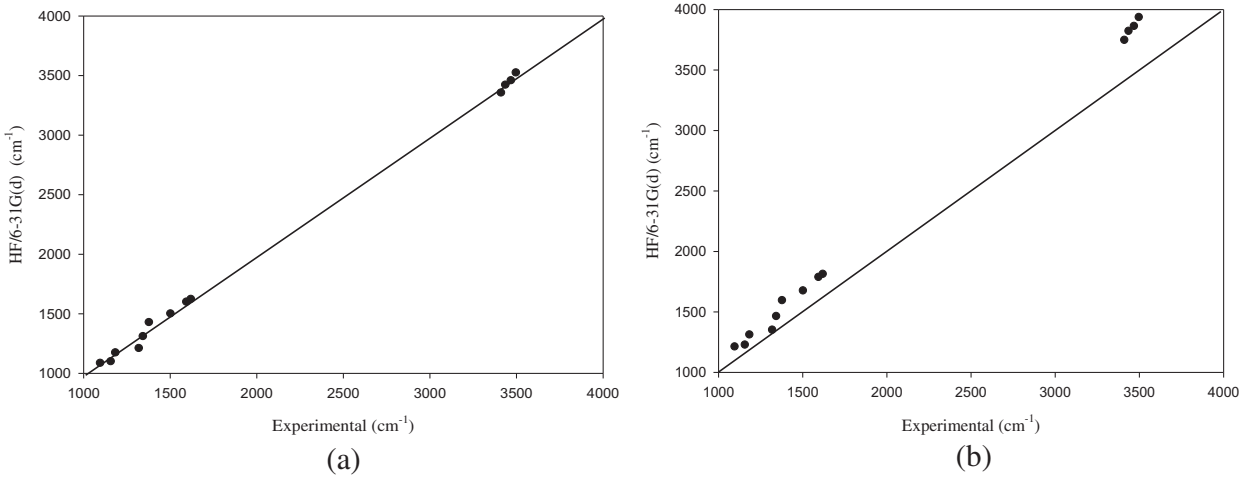

Fig. 4. Comparison of theoretical ($CHCl_3$) and experimental ($CDCl_3$) frequency (cm^{-1}) of sulfanilamide. (a) Scaled. (b) Unscaled.

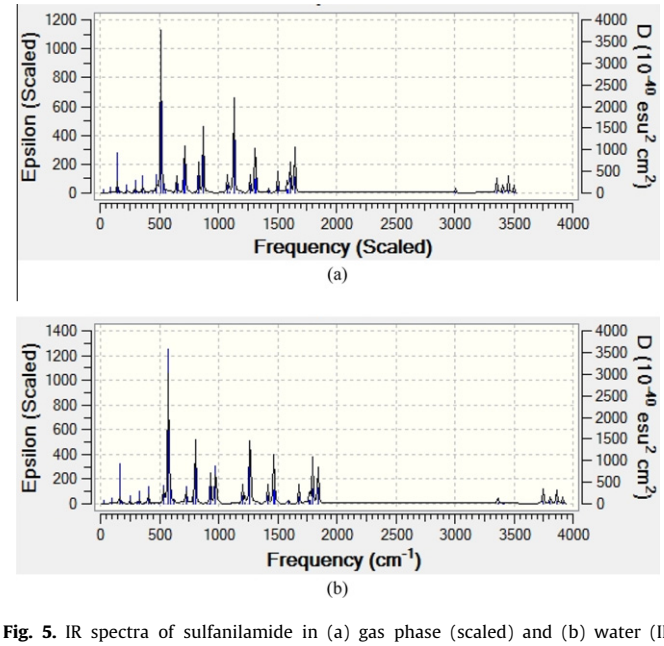

Fig. 5. IR spectra of sulfanilamide in (a) gas phase (scaled) and (b) water (IR intensities divided by the refractive index) at the HF/6-31G(d).

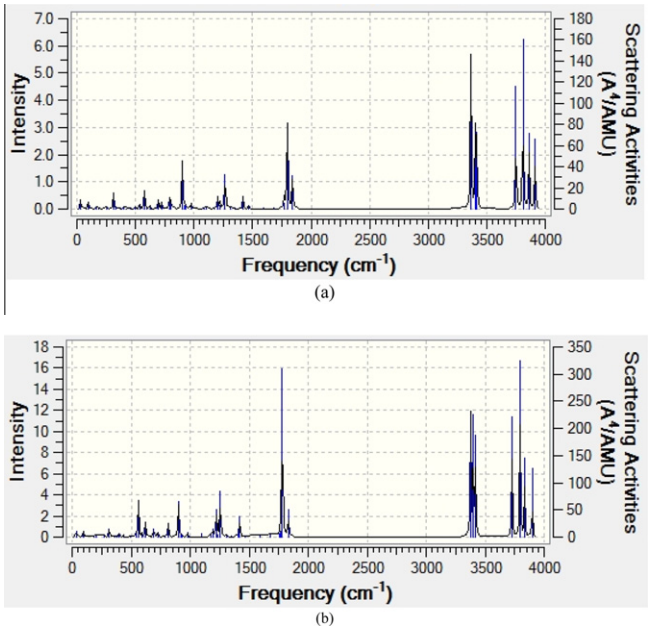

Fig. 6. Raman spectra of sulfanilamide in (a) gas phase and (b) water at the HF/6-31G(d).

systematic trend is observed in SMD. In PCM, no substantial change (1.3–2.1 kJ/mol) is observed for solvation free energies in the polar solvents but a quite distinguishable change is observed when SMD is employed. Increasing the dielectric constant from 2 to 2.2 yields a change of 0.8–2.5 kJ/mol for PCM and 6.3–7.1 kJ/mol for SMD. In both models, a significant change is observed in going from a non-polar to a polar solvent. Basis sets have no noticeable effect on the solvation energy for both models. Furthermore, solvation free energies at HF/6-31G(d) are more negative than that of MP2/6-31G(d) with PCM. For instance, solvation free energies at MP2/6-31G(d) increase by 7.9–8.9 kJ/mol for polar solvents whereas they increase by only 2.1–6.2 kJ/mol for non-polar solvents. For all solvents, SMD gives relatively higher solvation energies than that of PCM. For non-polar and polar solvents, the solvation free energy in SMD is higher by 9.6–19.7 kJ/mol and 15.5–33.0 kJ/mol, respectively than that of PCM. Experimental analysis [30] shows that sulfanilamide is more soluble in polar solvents and less soluble in non-polar solvents and it is interesting to note that a similar observation is found in this study. Our theoretical results revealed that solubility of sulfanilamide is decreased in the order H_2O > DMSO > CH_3CN > MeOH > $CHCl_3$ > CCl_4 > C_6H_{12} using PCM but there is no systematic order found for SMD.

The dipole moment is expected to be larger in solution than the corresponding dipole moment in the gas phase. Table 11 presents the dipole moments computed in the gas phase and different solvents (H_2O, DMSO, CH_3CN, MEOH, $CHCl_3$, CCl_4, C_6H_{12}) at the different level of theories (HF, B3LYP and MP2) and basis sets using PCM and SMD solvation models. All the calculated dipole moments in the gas phase are larger than the experimental value [31], however, the dipole moment at B3LYP/6-31G(d,p) is close to the experimental value. The difference between experimental dipole moments and those calculated at B3LYP with different basis sets vary from 0.13 to 0.19 Debye, whereas for HF it ranges from 0.29 to the 0.51 Debye. From lower to higher dielectric, the dipole moment increases gradually regardless of the theory or basis set. In addition, from small to larger basis sets the dipole moments increased smoothly at HF and B3LYP for both solvation models. The increase in dipole moment on going from gas to non-polar solvents range from 10% to 26% and to polar solvents they range from 25% to

Table 10
Solvation free energy (kJ/mol) of sulfanilamide in different solvents with PCM and SMD.

ϵ	PCM											SMD			
	6-31G(d)			6-31G(d,p)		6-31+G(d)		6-31+G(d,p)		6-311+G(d,p)		6-31G(d)		6-31G(d,p)	
	HF	B3LYP	MP2	HF	B3LYP	HF	B3LYP	HF	B3LYP	HF	B3LYP	HF	B3LYP	HF	B3LYP
78.3	−57.0	−48.5	−48.1	−56.7	−47.7	−57.0	−51.8	−55.6	−50.2	−57.7	−49.0	−90.0	−72.0	−88.7	−72.8
46.8	−56.1	−47.7	−47.3	−55.6	−47.3	−56.1	−50.6	−54.8	−49.4	−57.0	−48.1	−72.8	−63.6	−72.4	−62.8
35.6	−55.6	−47.3	−47.7	−54.8	−46.4	−55.2	−50.2	−54.0	−49.0	−56.1	−47.3	−77.0	−67.4	−76.6	−67.0
32.6	−55.2	−46.9	−46.4	−54.8	−46.4	−55.2	−49.8	−54.0	−48.5	−55.6	−47.3	−85.3	−72.1	−85.3	−70.3
4.7	−39.7	−34.7	−33.5	−39.3	−34.3	−39.0	−35.1	−37.2	−33.9	−39.3	−32.6	−59.0	−51.0	−59.0	−51.0
2.2	−24.3	−20.5	−20.5	−23.8	−20.5	−22.6	−21.3	−21.3	−20.5	−23.4	−19.2	−39.7	−35.1	−39.7	−34.7
2	−21.8	−18.4	−19.7	−21.3	−18.8	−20.1	−18.8	−18.8	−18.0	−21.0	−16.7	−32.6	−28.4	−32.6	−28.4

Table 11
Dipole moment (Debye) of sulfanilamide in gas phase and in different solvents using PCM and SMD.

	6-31G(d)		6-31G(d,p)		6-31+G(d)		6-31+G(d,p)		6-311+G(d,p)		6-31G(d)		6-31G(d,p)		Expt[a]
	HF	B3LYP	HF	B3LYP	HF	B3LYP	HF	B3LYP	HF	B3LYP	HF	B3LYP	HF	B3LYP	
Gas	6.33	5.97	6.33	5.95	6.11	5.97	6.17	5.99	6.25	6.01	–	–	–	–	5.82
	PCM										SMD				
H20 (78.3)	8.58	8.53	8.65	8.57	8.82	9.06	8.89	9.09	8.95	9.09	9.52	9.52	9.61	9.57	–
DMSO (46.8)	8.55	8.49	8.61	8.53	8.79	9.02	8.85	9.05	8.91	9.05	8.57	8.55	8.63	8.59	–
CH3CN (35.6)	8.53	8.47	8.59	8.50	8.75	8.98	8.82	9.01	8.88	9.01	8.63	8.60	8.59	8.65	–
MEOH (32.6)	8.52	8.45	8.58	8.49	8.74	8.97	8.81	9.00	8.86	9.00	9.41	9.45	9.50	9.45	–
CHCl3 (4.7)	7.90	7.79	7.96	7.83	8.02	8.14	8.08	8.17	8.15	8.18	8.05	7.97	8.10	8.01	–
CCl4 (2.2)	7.31	7.10	7.35	7.12	7.34	7.34	7.39	7.36	7.45	7.37	7.35	7.16	7.40	7.19	–
C6H12 (2.0)	7.21	6.99	7.24	7.00	7.22	7.21	7.27	7.23	7.33	7.24	7.25	7.06	7.30	7.08	

[a] Ref. [29].

37%. Moreover, SMD provides relatively higher values for the dipole moment than PCM.

4. Conclusions

Our results indicate that in the gas phase, all calculated bond distances are significantly longer than the experimental results where hydrogen is present and significant differences are observed in some bond angles (containing N and S) and fell in the range 2.4–8.0°. Medium effect on bond distances and angles of sulfanilamide is small but it has significant effect on dihedral angles where changes range from 3.1° to 45.9°. Although the vibrational frequencies of solvated sulfanilamide do not change remarkably, significant change is observed for IR intensities and Raman scattering activities. Solvation free energies sharply increase in going from lower to higher dielectric constant for PCM regardless of the theories and basis sets but no systematic trend is observed in SMD. SMD gives relatively higher solvation energies (9.6–19.7 kJ/mol for non-polar and 15.5–33.0 kJ/mol for polar solvent) than that of the PCM. Furthermore, in polar media, PCM contribute no distinguishable change for solvation free energies and dipole moments.

Acknowledgment

We would like to thank Natural Sciences and Engineering Council of Canada (NSERC) for financial support. For providing necessary support and computer time, we also gratefully acknowledge the Atlantic Computational Excellence Network (ACEnet) funded by the Canada Foundation for Innovation (CFI), the Atlantic Canada Opportunities Agency (ACOA), and the provinces of Newfoundland & Labrador, Nova Scotia, and New Brunswick.

Appendix A. Supplementary data

Supplementary data associated with this article can be found, in the online version, at doi:10.1016/j.theochem.2010.08.027.

References

[1] S. Corni, C. Cappelli, R. Cammi, J. Tomasi, J. Phys. Chem. A 105 (2001) 8310.
[2] (a) J. Tomasi, in: B. Mennucci, R. Cammi (Eds.), Continuum Solvation Models in Chemical Physics: From Theory to Applications, John Wiley & Sons Ltd., England, 2007 (pp.6 and 167);
(b) C. Cappelli, in: B. Mennucci, R. Cammi (Eds.), Continuum Solvation Models in Chemical Physics: From Theory to Applications, John Wiley & Sons Ltd., England, 2007 (pp. 6 and 167).
[3] J. Wang, W. Wang, S. Huo, M. Lee, P.A. Kollman, J. Phys. Chem. B 105 (2001) 5055.
[4] D.S. Cerutti, N.A. Baker, J.A. McCammon, J. Chem. Phys. 127 (2007) 155101.
[5] C.J. Cramer, D.G. Truhlar, Chem. Rev. 99 (1999) 2161.
[6] L. Onsager, J. Am. Chem. Soc. 58 (1936) 1486.
[7] D. Rinaldi, L. Rivail, Theor. Chem. Acc. 32 (1973) 57.
[8] J. Tomasi, M. Persico, Chem. Rev. 94 (1994) 2027.
[9] J.L. Rivail, D. Rinaldi, M.F. Luiz-Lopez, in: J. Lecszynski (Ed.), Computational Chemistry: Review of Current Trends, World Scientific, Singapore, 1995.
[10] M. Cossi, N. Rega, G. Scalmani, V.J. Barone, Chem. Phys. 114 (2001) 5691.
[11] S. Miertus, E. Scrocco, J. Tomasi, Chem. Phys. 55 (1981) 117.
[12] A. Topacli, B. Kesimli, Sepctrosc. Lett. 34 (2001) 513.
[13] <http://nobleprize.org/nobel_prizes/medicine/laureates/1939/domagk-bio.html> (accessed June 16, 2010).
[14] J.B. Mueller, M. Wall, Spectrochim. Acta, Part A 23 (1967) 2465.
[15] C. Topacli, A. Topacli, J. Mol. Struct.: THEOCHEM 644 (2003) 145.
[16] H.T. Varghese, C.Y. Panicker, D. Philip, Spectrochim. Acta, Part A 65 (2006) 155.
[17] A.D. Popova, M.K. Georgieva, O.I. Petrov, K.V. Petrov, E.A. Velcheva, Int. J. Quantum Chem. 107 (2007) 1752.
[18] M.J. Frisch, G.W. Trucks, H.B. Schlegel, G.E. Scuseria, M.A. Robb, J.R. Cheeseman, G. Scalmani, V. Barone, B. Mennucci, G.A. Petersson, H. Nakatsuji, M. Caricato, X. Li, H.P. Hratchian, A.F. Izmaylov, J. Bloino, G. Zheng, J.L. Sonnenberg, M. Hada, M. Ehara, K. Toyota, R. Fukuda, J. Hasegawa, M. Ishida, T. Nakajima, Y. Honda, O. Kitao, H. Nakai, T. Vreven, J.A. Montgomery Jr., J.E. Peralta, F. Ogliaro, M. Bearpark, J.J. Heyd, E. Brothers, K.N. Kudin, V.N. Staroverov, R. Kobayashi, J. Normand, K. Raghavachari, A. Rendell, J.C. Burant, S.S. Iyengar, J. Tomasi, M. Cossi, N. Rega, J.M. Millam, M. Klene, J.E. Knox, J.B. Cross, V. Bakken, C. Adamo, J. Jaramillo, R. Gomperts, R.E. Stratmann, O. Yazyev, A.J. Austin, R. Cammi, C. Pomelli, J.W. Ochterski, R.L. Martin, K. Morokuma, V.G. Zakrzewski, G.A. Voth, P. Salvador, J.J. Dannenberg, S. Dapprich, A.D. Daniels, O. Farkas, J.B. Foresman, J.V. Ortiz, J. Cioslowski, D.J. Fox, Gaussian 09, Revision A.02, Gaussian, Inc., Wallingford CT, 2009.
[19] A.V. Marenich, C.J. Cramer, D.G. Truhlar, J. Phys. Chem. B 113 (2009) 6378.
[20] J.P. Merrick, D. Moran, L. Radom, J. Phys. Chem. A 111 (2007) 11683.
[21] R.D. Dennington II, T.A. Keith, J.M. Millam, GaussView 5.0, Wallingford, CT, 2009.
[22] R.R. Pappalardo, E.S. Marcos, M.F. Ruiz-López, J. Am. Chem. Soc. 115 (1993) 3722.
[23] E. Shefter, P. Sackman, J. Pharm. Sci. 60 (1971) 282.

[24] W.J. Hehre, L. Radom, P.v.R. Schleyer, J.A. Pople, Ab Initio Molecular Orbital Theory, first ed., Wiley, New York, 1986.
[25] N.P.G. Roeges, A Guide to the Complete Interpretation of Infrared Spectra of Organic Structure, first ed., Wiley, England, 1994.
[26] J.A. Pople, A.P. Scott, M.W. Wong, L. Radom, Isr. J. Chem. 33 (1993) 345.
[27] M.D. Halls, H.B. Schlegel, J. Chem. Phys. 109 (1998) 10587.
[28] R. Cammi, C. Cappelli, S. Corni, J. Tomasi 104 (2000) 9874.
[29] C.J. Cramer, Essential of Computational Chemistry, second ed., Wiley, England, 2004.
[30] A. Weizmann, J. Am. Chem. Soc. 70 (1948) 2342.
[31] W.D. Kulmer, I.F. Halverstantd, J. Am. Chem. Soc. 63 (1941) 2182.